Potential reduction of concrete deterioration through controlled DEF in hydrated concrete

academicJournals

Vol. 8(24), pp. 1307-1318, 30 June, 2013
DOI: 10.5897/IJPS2013.3923
ISSN 1992 - 1950 © 2013 Academic Journals
http://www.academicjournals.org/IJPS

International Journal of Physical Sciences

Full Length Research Paper

Potential reduction of concrete deterioration through controlled DEF in hydrated concrete

Samo Lubej[1] and Milan Radosavljevic[2]

[1]Faculty of Civil Engineering, University of Maribor, Smetanova 17, 2000 Maribor, Slovenia.
[2]School of Construction Management and Engineering, University of Reading, Whiteknights, P. O. Box 219, Reading, RG6 & AW, United Kingdom.

Accepted 21 June, 2013

Delayed ettringite formation (DEF) is a chemical reaction with proven damaging effects on hydrated concrete. Ettringite crystals can cause cracks and their widening due to pressure on cracked walls caused by the positive volume difference in the reaction. Concrete may show improvements in strength at early ages but further growth of cracks causes widening and spreading through the concrete structure. In this study, finely dispersed crystallization nuclei achieved by adding air-entraining agent (AEA) and short vibration of specimens is presented as the main prerequisite for reducing DEF-induced deterioration of hydrated concrete. The study presents the method and mechanism for obtaining the required nucleation. Controlling long-term DEF by providing AEA-induced crystallisation nuclei, prevented excessive and rapid initial strength improvements, and resulted in a slight increase of compressive strength of fine grained concrete with only marginally lower density.

Key words: Delayed ettringite formation (DEF), aerated concrete, strength improvement.

INTRODUCTION

Delayed ettringite formation in cementitious materials is considered a harmful chemical reaction leading to a variety of damages (Diamond, 1996; Thomas, 2001; Barbarulo et al., 2005). The volume of the formed DEF crystals in the hardened concrete is larger than the volume of reactants and the main results are forces from the growing crystals acting upon walls of the crack. As a consequence, DEF cracks continue getting wider and spread through the concrete structure (Sahu and Thaulow, 2004; Thomas et al., 2008). In the study of DEF on railroad ties, Sahu and Thaulow (2004) found massive ettringite deposits at the interface between the paste and aggregate but with no signs of alkali-silica reaction, DEF was found to be the sole reason for map cracking. However, recent research has led to a better understanding of the mechanisms of DEF. It is believed that internal sulphate attack (ISA), which occurs in an environment free from external sources of sulphate, is the main mechanism that leads to DEF, particularly for heat-cured concrete structures (Collepardi, 2003).

In general, it is acknowledged that DEF is a result of a number of factors and conditions including excessive temperatures of above 70°C, the presence of sulfates, existing cracks, moist conditions etc (Taylor, 1990; Lawrence, 1995a, b; Ekolu et al., 2007a). Ekolu et al. (2007b) summarise various control measures that could be used for prevention of DEF, including the use of chemical additives. However, preventative measures and improvements in general durability require further attention.

In practice concrete and mortar mixes are normally based on Portland cement clinker, where the chemical process of hydration of clinker minerals yields hydrates and hydroxides. Because of the presence of gypsum, the

*Corresponding author. E-mail: samo.lubej@um.si. Tel. +386 2 2294333, Fax. +386 2 2524179.

chemical reaction between tricalcium aluminate (C_3A), gypsum ($CaSO_4$, $2H_2O$) and water, forms ettringite crystals ($3CaO$, Al_2O_3, $3CaOSO_4$, $31H_2O$). The volume difference in this reaction is positive and ettringite crystals grows faster, quickly growing on the unhydrated cement particles, which can slow down the hydration (Swaddiwudhipong et al., 2002). The presence of ettringite in a liquid cementitious system is unproblematic but its formation or re-formation in already hydrated concrete can lead to extensive damages (Collepardi, 2003). Due to the resulting volume difference particularly in the presence of sulfates, an expansive force within concrete can cause its disintegration (sulfate corrosion). It is well known that cements with low C_3A content are more resilient to sulfate corrosion although this also depends on the form of C_3A (Mather, 1968). For instance, crystalline C_3A is more reactive than its amorphous version.

The positive volume difference as a result of early ettringite formation (EEF) in cementitious materials rich with $C_4A_3\bar{S}$ calcium aluminate sulphate (expansive cement) can be used to compensate for the shrinkage during drying (Collepardi, 2001). In this case $C_4A_3\bar{S}$ hydrates within a few hours or days producing uniform distribution of ettringite and homogeneous expansion of hardened concrete at early stages. However, it is less known that ettringite could be formed in hardened cementitious materials without causing the well documented damages, which could potentially lead to their controlled strengthening.

The formation of a new phase characterized by volume expansion for the purpose of strength improvement is well known in the mainstream material science literature (Mishnaevsky, 2007). Such strengthening is based upon the creation of the internal compressive stresses on the contact between the existing matrix and the new phase particles, and depends on their shape, size and overall dispersion (Clifton and Ponnersheim, 1994). The newly formed particles should be small, spherical and located sufficiently apart from each other to avoid overlapping stress fields. Strength improvement of the Al_2O_3 ceramics with finely dispersed ZrO_2 particles is one example of this kind of strengthening (Cutler et al., 1987; Marshall et al., 1991). Internal stresses in the Al_2O_3 matrix created by applying the external force trigger polymorphic transformation of a tetragonal crystalline structure of ZrO_2 into a monoclinic crystalline structure. Increased volume creates substantial compressive stresses in the matrix surrounding the transformed particles leading to a several fold increase in compressive strength as well as resistance to the spreading of cracks. Studies that apply mechanisms of this kind for strength improvement of concrete are rare (Sobolev et al., 2006).

The creation of internal compressive stresses around particles or nuclei that have been transformed is the key requirement for such transformational strengthening. Its intensity depends on particle morphology, size and dispersion. Ideally, the particles should be small, spherical and uniformly dispersed to avoid overlapping their stress fields.

MATERIALS AND METHODS

In this study, the authors provide an investigation of a type of controlled DEF that may prevent deterioration or perhaps improve mechanical properties of hydrated fine grained concrete. A microstructure where crystallization nuclei are formed as a result of adding finely dispersed air-entraining agent (AEA) is the key prerequisite for such improvements. It is assumed that this would lead to localized and controlled formation of ettringite crystals, which could prevent DEF-induced deterioration. Their size and distribution depends on the level of dispersion of added AEA. The formation of localized ettringite crystals in the nuclei, particularly those adjacent to cracks, creates beneficial internal compressive stresses as the ettringite fills the nuclei. Similar to strength improvement of the Al_2O_3 ceramics described above, these internal compressive stresses lead to closure of nearby cracks preventing the growth of ettringite crystals. Furthermore, Ryu and Otsuki, (2002) show that the closure itself is beneficial since it decreases concrete permeability.

On the whole the experiments were based on fine grained concrete mixes using one type of cement, one type of AEA, fly ash and sand according to EN 196-1. Water-cement ratio, quantities of additives and hydration conditions were determined through laboratory testing. In addition, the experiments were based on specific climatic conditions necessary to achieve a controlled DEF in hydrated concrete. The investigation was based on four Portland cement (PC) CEM I 42, 5 R fine grained concrete mixes presented in Table 1.

The objective of this study is to investigate whether controlled DEF could lead to the reduction of deterioration and potential strengthening of hydrated fine grained concrete. To achieve this objective the study involves the following methods:

(1) Exposing hardened fine grained concrete prisms from the mix BI to the Duggan's test (Grabowski et al., 1992) (that is, prisms BI-DT); the test is essentially a cyclical interplay of heating and humidity and consists of a number of phases: prisms were first immersed in demineralised water for 72 h at 20 ± 2°C followed by 24 hours of drying in a drying chamber at 81 ± 2°C; they were then again immersed in the demineralised water for 24 h at 20 ± 2°C before being subject to 24 h drying in the chamber at 81 ± 2°C; in the last phase, prisms were immersed in the demineralised water for 24 h at 20 ± 2°C and then dried in the chamber for 72 h at 81 ± 2°C; the prisms were laboratory conditioned for 48 h in desiccators in between each of the above phases, and were once again immersed in the demineralised water for 24 h in order to fill the capillaries and voids with water,
(2) Strength comparison between hardened concrete prisms from mixes A, B, BI and prisms from mix BI that were exposed to the Duggan's test,
(3) Measuring ettringite formation by monitoring the length change (expansion) with a digital micrometer,
(4) microstructure comparison between hardened fine grained concrete samples from mixes A and AI where ettringite crystals were not detected with samples that were exposed to Duggan's test using electronic microscopy (that is, samples B-DT and BI-DT),
(5) Chemical analysis of ettringite crystals from samples B-DT and BI-DT in order to determine mass and atomic quantities of individual elements.

Four different mixes (A and AI, B and BI) were used for

Table 1. The four fine grained concrete mixes under investigation.

Parameter	Mix A (g)	Mix AI (g)	Mix B (g)	Mix BI (g)
Water	250	218,2	225	218,2
PC	450	450	310	310
Fly ash	-	-	140	140
AEA	-	6,8	-	6,8
Standard sand EN 196-1	1350	1350	1350	1350

Table 2. Results of the laboratory analysis for fly ash components.

Component part	Content (%)
Loss on ignition	0.41
Insoluble residue	16.67
SiO_2 impure	13.08
SiO_2 pure	47.62
SiO_2 soluble	0.64
SiO_2 total	48.26
SiO_2 active	35.18
Cao active	7.56
SO_3	1.88
CaO free	2.00

Figure 1. Apparatus for the measurement of length change of hardened concrete according to ASTM C490-86 placed in a climatic chamber.

comparative purposes because variations carried on:

(1) AEA content (A and B without AEA, versus AI and BI with AEA)
(2) Fly ash content (A and AI without fly ash versus B and BI with fly ash).

The comparison is necessary to identify the potential impact AEA and fly ash may have on mechanical properties before the prisms are exposed to Duggan's test (e.g. undesirable loss of compressive strength).

The above fine grained concrete mixes were prepared using a laboratory mixer according to EN 196-1. The conformity of fly ash for concrete was tested according to EN 450-1. The laboratory analysis of components presented in Table 2 confirmed that the fly ash used fulfils the criteria set in EN 197-1. Prisms were cast using 40 × 40 × 160 mm steel moulds. The samples from the mix B without AEA were then vibrated for 120 seconds with a standard low frequency of 50Hz and amplitude of 0.75 mm. The AEA-based samples from mixes AI and BI were vibrated for only 5 seconds under the same standard vibrating conditions as mix B samples in order to keep the volume of entrained air at an acceptable level (that is, preventing excessive reduction of strength). Past research shows that AEA-based samples should be vibrated with caution. For instance, Crawley (1953) found that high-frequency vibration causes more rapid loss of entrained air than moderate or low frequency vibration, and Hover (2001) reports that excessive vibration may lead to a complete loss of entrained air.

On the other hand, it has been found that short vibration cycles can improve compressive strength of concrete (Ozyldirim and Lane, 2003). A much shorter low-frequency vibration was therefore adopted to avoid a complete loss of finely dispersed crystallisation nuclei required for the controlled DEF. Controlled DEF is achieved by providing space for growth of ettringite crystals in the AEA-induced nuclei without any harm to hardened concrete. Specific climatic conditions were achieved by curing all prisms for 28 days in a climatic chamber at a temperature of 20±2°C and relative humidity of 98±2%. After a required 28-day curing period six prisms from each of the mixes B and BI were exposed to Duggan's test in order to achieve the accelerated ettringite formation. The prisms were then placed into a standard apparatus for the determination of length change of hardened cement paste, mortar and concrete, constructed according to ASTM C490-86. During these measurements the apparatus itself was placed in the climatic chamber with a constant temperature of 20±2°C and relative humidity of 98±2% shown in Figure 1.

Ettringite formation was then monitored by measuring length change (expansion) with Mahr's MarCator 1080/12.5/0.005 mm digital micrometer. The results were recorded with an analogue/digital converter connected to a workstation. Developing expansion was measured regularly in 15 m intervals with a measurement accuracy of 0.005 mm, although intervals could well be longer considering the slow pace of DEF.

Density of hardened fine grained concrete (ρ), its compressive (f_c) and flexural strength (f_m) were measured on 10 additional prisms for each of the three mixes after standard 7, 14 and 28 days, and additionally after 56 and 121 days when compressive and flexural strengths should reach a plateau. Mechanical properties of fine grained concrete were examined with a universal dynamometer and a method according to EN 196-1. Optical microscopy using OLYMPUS SZX stereo microscope and QUANTA 200 3D electronic microscope was used to monitor the microstructure development in the hydrated fine grained concrete. The use of the latter enables longer low-vacuum observations without gold or carbon coating of samples. Chemical analysis of reactants in the hydrated paste was performed with Line Scan Microscopy (LSM) using SIRION 400 NC scanning electron microscope that works at high-vacuum but

Table 3. Densities and mechanical properties of hardened fine grained concrete (mix A).

Time interval (days)	ρ (kg/m^3)	f_m (MPa)	f_c (MPa)
121	1894	6.1	26.4

Table 4. Densities and mechanical properties of hardened fine grained concrete (mix AI).

Time interval (days)	ρ (kg/m^3)	f_m (MPa)	f_c (MPa)
7	1876	4.0	18.0
14	1904	4.4	21.8
28	1883	7.2	23.3
56	1885	7.3	23.5
121	1887	7.4	25.5

Table 5. Densities and mechanical properties of hardened fine grained concrete (mix B).

Time interval (days)	ρ (kg/m^3)	f_m (MPa)	f_c (MPa)
7	1860	3.2	11.9
14	1857	3.5	14.2
28	1868	3.9	17.4
56	1872	4.1	19.3
121	1866	5.6	22.1

Table 6. Densities and mechanical properties of hardened fine grained concrete (mix BI).

Time interval (days)	ρ (kg/m^3)	f_m (MPa)	f_c (MPa)
7	1801	2.7	11.6
14	1807	5.2	14.3
28	1803	4.1	17.7
56	1805	4.1	17.8
121	1818	5.6	21.0

specimens have to be dry and treated (carbon treatment in this case). The ettringite crystals were characterised with the Energy Dispersive X-Ray (EDX) spectroscopy using JEOL JSM 5610 scanning electron microscope operated at 20kV for single-point 100 s long EDX measurements.

RESULTS AND DISCUSSION

Tables 3, 4, 5 and 6 show measured densities, flexural f_m and compressive strength f_c of hardened fine grained concrete prisms for mixes A, AI, B and BI that were not exposed to Duggan's test. The compressive strength of AI (BI) prisms after 121 days is only 3.4 % (5 %) lower than that of prisms A (B), which indicates that loss of strength due to added AEA can be prevented with short low-frequency vibration. These results reveal that 5 s vibration of BI prisms was sufficient to achieve a minimum loss of mechanical properties, which is normally expected from added AEA. On the other hand, the short vibration interval prevents the loss of crystallisation nuclei that can be seen later in the text.

Tables 7 and 8 show measured densities and mechanical properties of hardened fine grained concrete prisms for mortar mixes B and BI, but this time after 121 days, and exposed to Duggan's test after 28 days. Flexural strength of prisms B-DT that were exposed to Duggan's test has almost doubled to 11.2MPa, and compressive strength has more than doubled as well. These substantial increases in strength were not expected but to some extent there are some parallels with a study by Zhang et al. (2008). The study show that growth of ettringite crystals in a limited space of microvoids

Table 7. Density and mechanical properties of hardened fine grained concrete (B-DT: mix B exposed to Duggan's test).

Time (days)	ρ (kg/m^3)	f_m (MPa)	f_c (MPa)
121	2211	11.2	60.4

Table 8. Density and mechanical properties of hardened mortar prisms (BI-DT: mix BI with Duggan's test).

Time (days)	ρ (kg/m^3)	f_m (MPa)	f_c (MPa)
121	1810	6.0	22.4

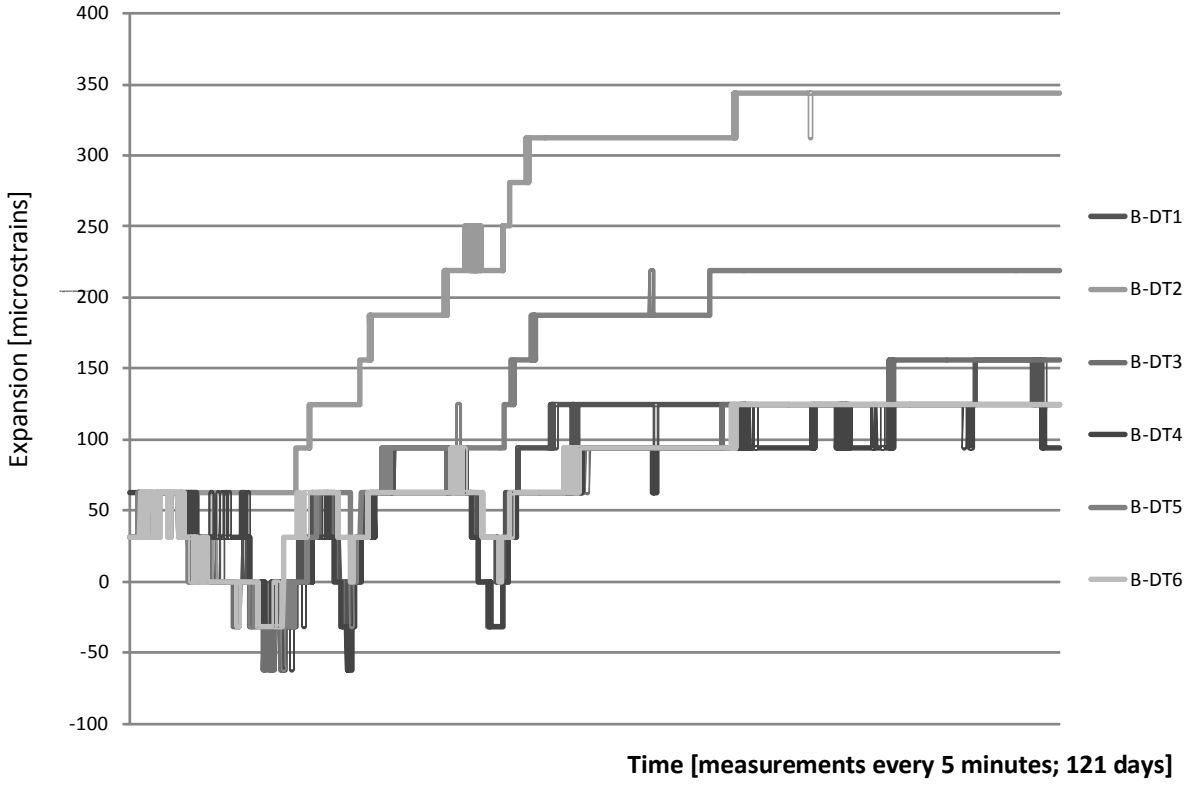

Figure 2. Change of length of six B-DT mortar prisms after the Duggan's test.

or preformed microcracks may lead to further evolution of localised microcracks. This process decreases the strength of prisms in early stages but ettringite crystals penetrate into the newly formed microcracks leading to partially recovered flexural strengths at later stages. One of the reasons for the increases could be associated with the increased ductility as a result of DEF-related expansion reported by Brunetaud et al. (2008). The observed causal relationship between tensile ductility and compressive strength has been observed in more detail by Bortolotti (1994). However, such increases are short-lived because the observed growth of ettringite crystals leads to the expansion at later stages, causing further cracking and deterioration of concrete.

Figures 2 and 3 show change of length for the six fine grained concrete prisms from the mixes B and BI that were exposed to Duggan's test and a final 24 hour immersion in demineralised water. The change of length of prisms was recorded daily and stopped after 93 days when measurements did not show any further expansion.

Comparing microstructures of the specimens from fine grained concrete mixes A, AI, and BI presented in Figure 4a, b and c demonstrate that, as expected, similar AEA-induced nuclei exist in AI and BI specimens.

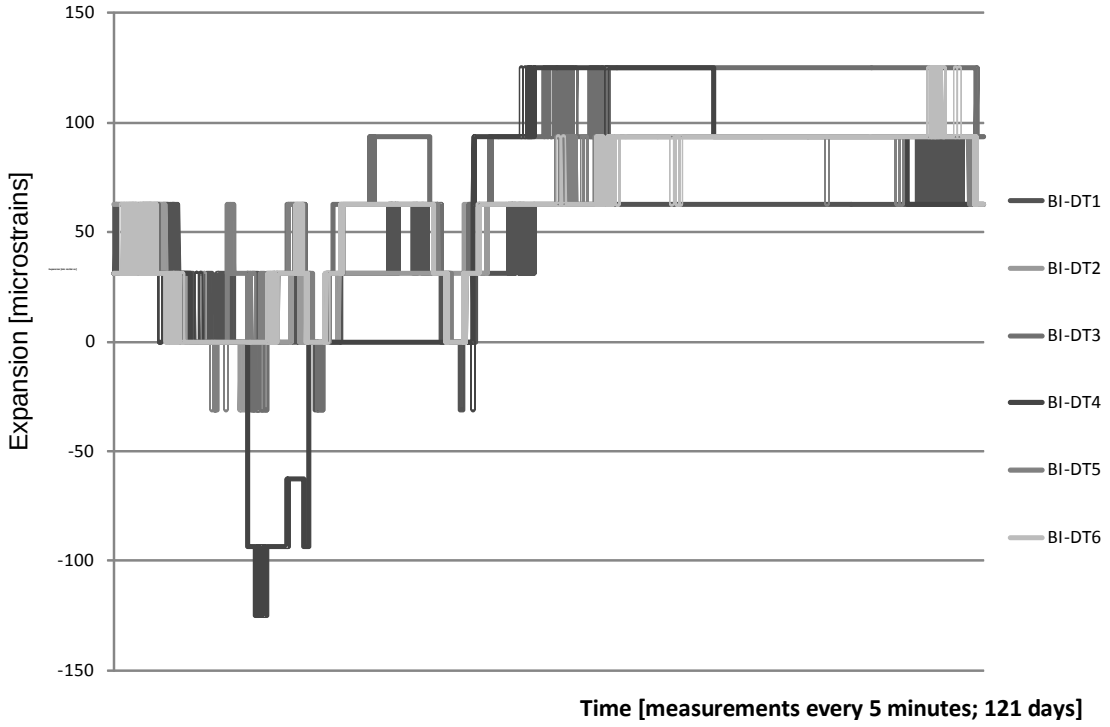

Figure 3. Change of length of six BI-DT fine grained concrete after the Duggan's test.

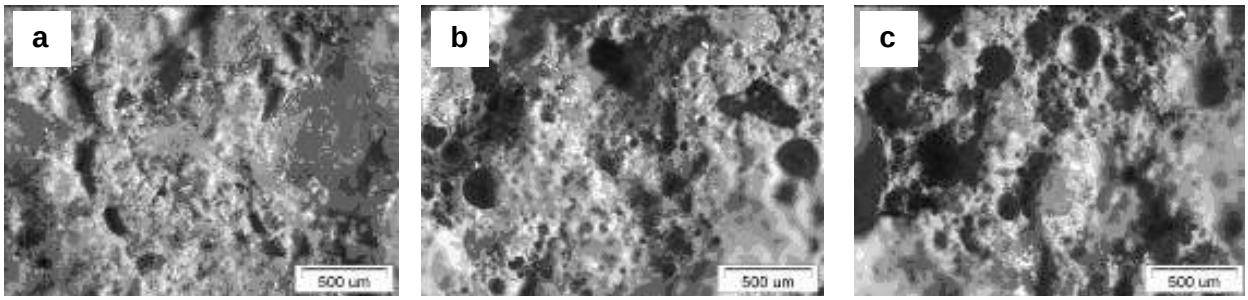

Figure 4 (a, b, c). Microstructures of fine grained concrete A, AI and BI after 121 days (500x magnification in all three cases; images obtained with OLYMPUS SZX stereo microscope).

Although ettringite crystals can be found in concretes produced by using pure Portland cement, no visible ettringite crystals were detected in any of the large number of prisms from the mix A. Ettringite crystals did appear in specimens of all other fine grained concrete mixes. Microstructures of specimen from the fine grained concrete mix AI show no visible ettringite crystals in AEA nuclei themselves displayed in Figure 5a, but they were detected in microcracks as seen in Figure 5b and c. Similar to Myneni et al. (1997) these crystals have thin, needle-shaped morphology and are approximately 2 µm in length revealing rapid growth. Fly ash in fine grained concrete mix BI may well be a source of soluble calcium for ettringite formation (Solem and McCarthy, 1992; Zhang and Reardon, 2003; Chrysochoou and Dermatas, 2006), because its crystals were found in greater quantities in microcracks and within the AEA-induced nuclei. Figure 6a, b, c and 7a, b, c, d, e, f show that ettringite crystals have thin, needle-shaped morphology but those found in microcracks are only approximately 2µm in length shown in Figure 7f, as opposed to 10 µm crystals found in the nuclei in Figure 6b.

The microcrack that appeared on the surface of a nucleous in Figure 7f can be associated with the shrinkage of the matrix during hydration (Stang, 1996). The comparison between various different BI specimen shows that ettringite crystals start growing wherever there is enough space for growth before further damaging

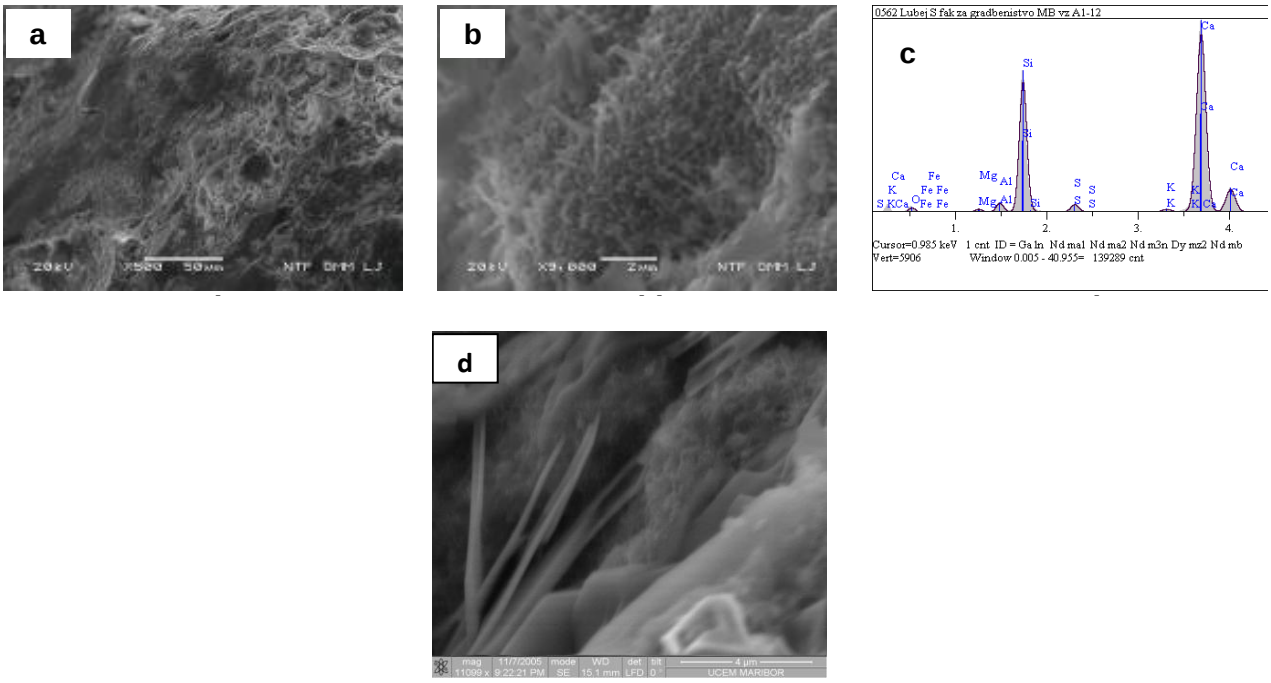

Figure 5 (a, b, c, d). Microstructure of fine grained concrete AI after 121 days (500x magnification in Figure 5a, and 9000x magnification of an area with thin approximately 2µm long ettringite crystals in figure 5b and 11000x magnification with QUANTA 200 3D electronic microscope in figure 5d; the results of the EDX analysis of a crystal from this area is in Figure 5c.

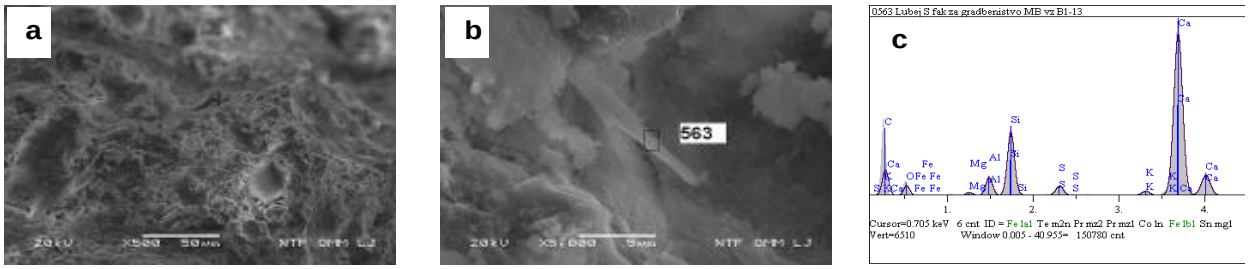

Figure 6 (a,b,c). Microstructure of fine grained concrete BI after 121 days (500x magnification in Figure 6a; the first studied area under 500x magnification of a nucleus with thin ettringite crystals with needle-shaped morphology and approximately 10um in length in figures 6b with the results of the EDX analysis of crystal 563 in Figure 6c).

concrete which enables further growth. AEA-induced nuclei may therefore act as relief reservoirs enabling the growth of substances like ettringite crystals in hardened concrete with minimum or no damaging effects. Hime, (1996) recommends air-entrainment as a way to prevent DEF and reports only a single incident where air-entrained concrete suffered from DEF.

Mix B has only been used to compare the microstructure and mechanical properties of specimen where fly ash has been added and the prisms were exposed to Duggan's test. Figure 8a reveals a microcrack in the B-DT sample at 500x magnification and Figure 8b clearly shows a cluster of up to 3 µm long ettringite crystals in the microcrack at 5000x magnification. Mehta (1983) reports that such type II crystals with the length of 1 to 2 µm and thickness of 0.1 to 0.2 µm are known to be more expansive and potentially more damaging than much longer - type I crystals. Because there are no AEA-induced nuclei DEF in B-DT samples increased microcracking giving space to further growth of ettringite crystals, which inevitably damage the hardened concrete. However, expansion of B-DT samples was not dissimilar to expansion of other samples. This may be assigned to a relatively short time interval since expansion was monitored for only 93 days after the Duggan's test.

Ettringite crystals growing in microcracks fill the empty space and press against their walls causing the DEF-induced expansion of concrete. As discussed earlier, this

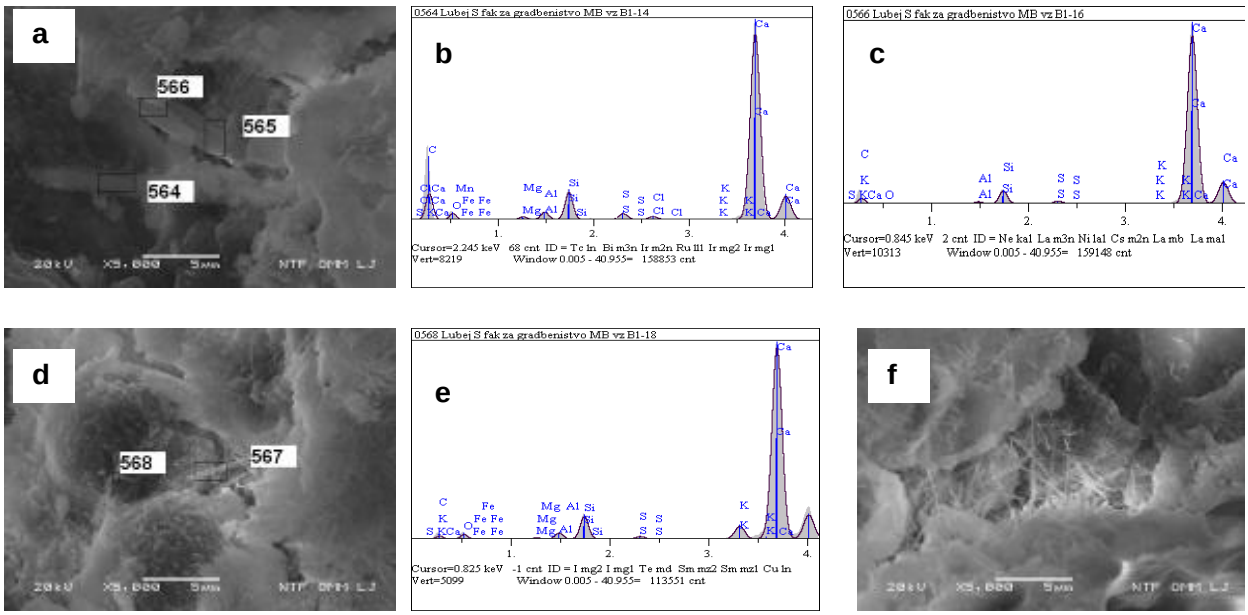

Figure 7 (a,b,c,d,e,f). Microstructure of fine grained concrete Bl after 121 days (the second studied area from figure 6a under 5000x magnification in Figure 7a,d and f; the results of the EDX analysis of crystal 564, 566 and 568 are in Figure 7b,c and e respectively).

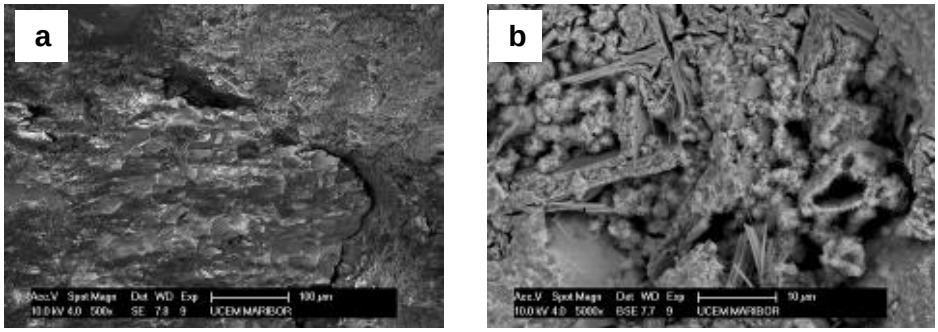

Figure 8 (a, b). Microstructure of fine grained concrete Bl after 121 days (500x magnification in figure 8a and 5000x magnification in Figure 8b; this mortar mix was used for comparative purposes only).

may in turn lead to initially improved mechanical properties before they are significantly reduced due to further evolution of growth-related microcracking. Compressive and flexural strength figures for B-DT samples after 121 days confirm this with compressive strength more than double the compressive strength of all other specimen. This improvement of mechanical properties is probably caused by ettringite crystals filling the empty space in existing microcracks before further evolution of localised microcracks that would significantly decrease the mechanical properties and damage concrete.

If DEF is limited to growth in microcrasks then specimens BI-DT that were exposed to Duggan's test should exhibit similar properties to B-DT specimens. Microstructure of the hardened fine grained concrete BI-DT after 121 days reveals visible ettringite crystals in AEA-induced nuclei in Figures 9b and 10b at 1,000 x and 5,000 x magnification respectively. These crystals are longer 10 µm type I crystals that are reportedly less damaging. The studied sections where AEA nuclei were present exposed some localised microcracking within the nuclei and presence of short ettringite crystals with needle-shaped morphology in the microcracks seen in Figure 11a and b. However, the majority of ettringite crystals were found within the nuclei themselves so the effect of their growth was assumed to be less damaging. Minimum expansion as shown in Figure 3 and comparable mechanical properties of specimens from all mixes, confirm this assumption.

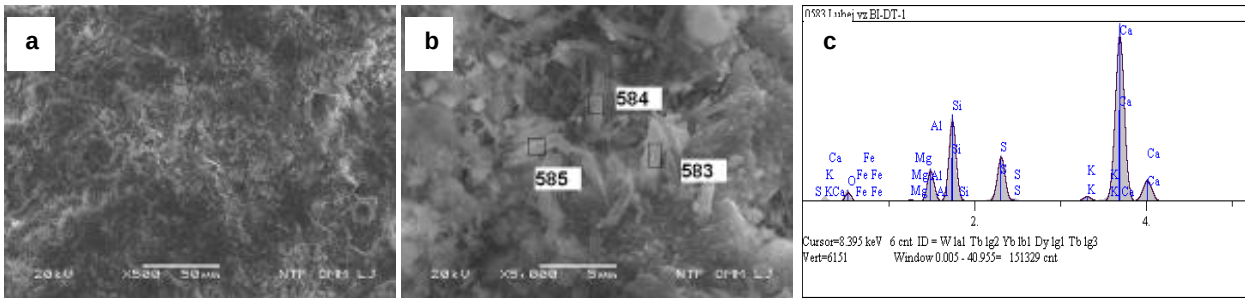

Figure 9 (a, b, c). Microstructure of fine grained concrete Bl after 121 days (500x magnification in Figure 8a with 5000x magnification of group crystals in the first studied area in figure 9b; the results of the EDX analysis of crystal 583 are in Figures 9c).

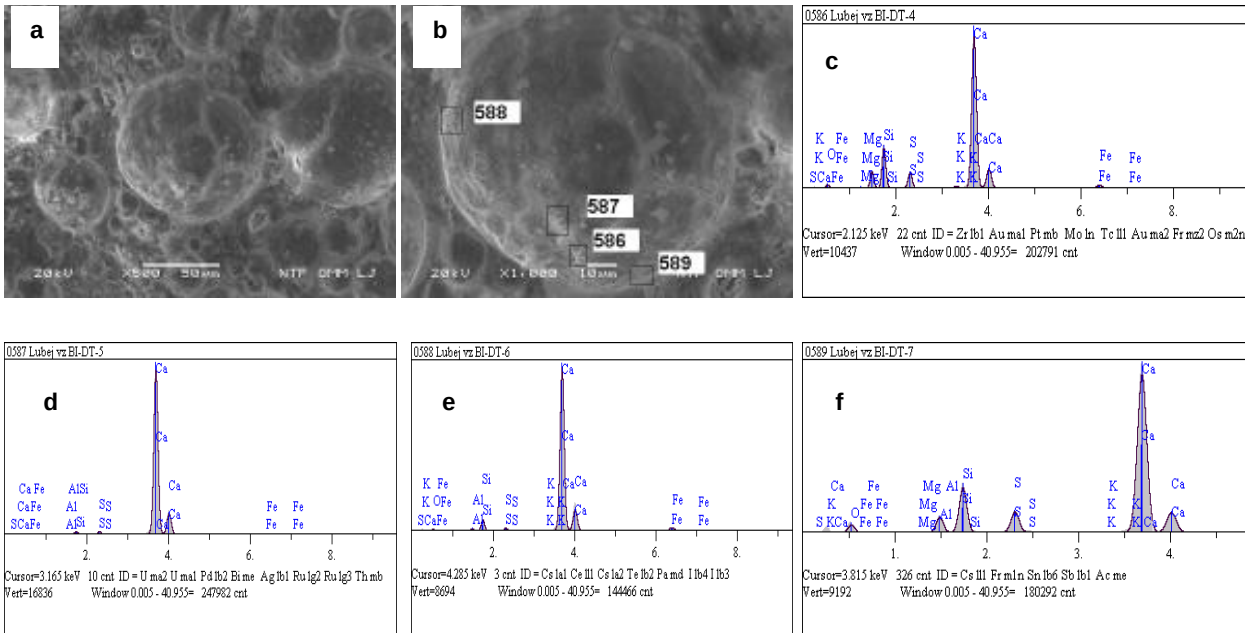

Figure 10 (a, b, c, d, e, f). Microstructure of fine grained concrete BI-DT after 121 days (500x magnification of a group of AEA-induced air voids in Figure 10a and 1000x magnification of an air void in Figure 10b; the results of EDX analysis of approximately 5 µm long crystals 586 and 587, and approximately 2 µm long crystals 588 and 589 are in Figures 7c, d, e and f respectively).

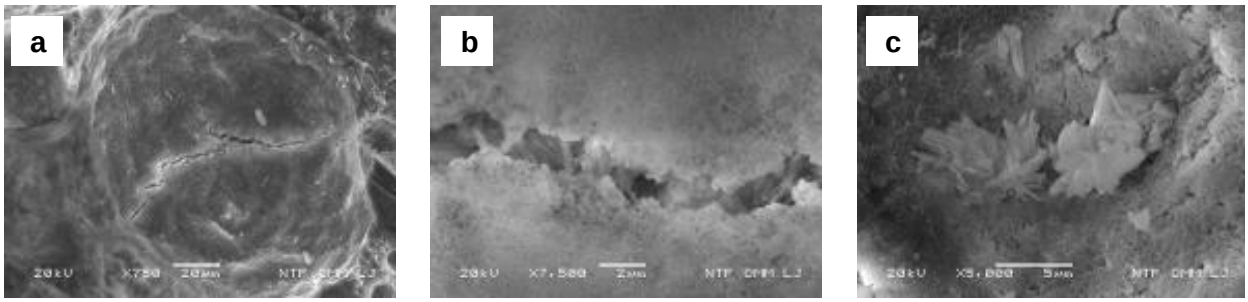

Figure 11 (a, b, c). Microstructure of fine grained concrete BI-DT after 121 days (750x magnification of an AEA nucleus with a microcrack in Figure 11a, 7,500x magnification of the microcrack in Figure 11b and 5000x magnification of the edge of the nucleus with a group of ettringite crystals in Figure 11c).

Table 9. Density and mechanical properties of hardened fine grained concrete without added AEA after 121 days for (prisms A, B and B-DT).

Variables	A	B	B-DT
ρ (kg/m^3)	1894	1866	2211
f_m (MPa)	6.1	5.6	11.2
f_c (MPa)	26.4	22.1	60.4

Table 10. Density and mechanical properties of hardened fine grained concrete with added AEA after 121 days for (prisms AI, BI and BI-DT).

Variables	AI	BI	BI-DT
ρ (kg/m^3)	1887	1818	1805
f_m (MPa)	5.6	5.6	6.0
f_c (MPa)	25.5	21.0	22.4

Table 11. EDX analysis results of the ettringite crystal at point 562 from sample AI in Figure 5c after 121 days.

Element	Mass %	Atomic %
Al	1.851	2.189
Si	26.567	30.187
S	1.740	1.732
Ca	55.105	43.878

The achieved compressive and flexural strengths of BI-DT specimens presented in Table 8 were similar to those of specimens B and BI in Tables 5 and 6 respectively and only 12% (15%) lower than those of specimens A(AI). The predominantly nuclei-based growth of ettringite crystals prevented excessive growth-related pressure on the walls of microcracks so no unusual initial improvements of mechanical properties were detected in the studied period. With a diameter of approximately 100 μm the nuclei offer sufficient space for ettrigite crystals to grow without causing progressive cracking and damaging the concrete.

Table 12.EDX analysis results of the ettringite crystal from the first studied area at point 563 from sample BI in Figure 6c after 121 days.

Element	Mass %	Atomic %
Al	2.975	2.280
Si	10.235	7.536
S	1.595	1.029
Ca	38.594	19.915

The EDX analysis was performed on a number of identified crystals to examine the presence of ettringite, which was confirmed in all cases. Tables 9-15 show compositions of studied ettringite crystals from Figures 5-11. The cement paste close to fly ash particles often contains CH crystals (Xu et al., 1993). It is therefore not unusual to see variations in Al/Ca and S/Ca ratios between different crystals that are presented in the tables. Wherever CH crystals are present Al/Ca and S/Ca ratios remain high (0.1-0.18 and 0.05-0.24 respectively). On the other hand, Al/Ca and S/Ca ratios are low at points where CH crystals are absent (0.01-0.05 and 0.01-0.04 respectively). Relatively high content of Si at some points follows high Al/Ca and S/Ca ratios in a similar way as shown by Richardson (2000). This could be associated with the availability of active SiO_2 in the fly ash although the values remain high even for specimens AI that do not contain fly ash. This, on the other hand, could also be associated with increasing concentrations of Si in the cement paste during hydration as reported by Rothstein et al. (2002).

Ettringite crystals have formed as a result of volumetrically expansive sulfate reaction in porous areas predominantly within AEA-induced nuclei, microcracks and microvoids in general. Because the solid product volume in this reaction is greater than the solid reactant volume, this has led to the creation of internal stresses in the ettringite growth areas. Their growth within the AEA-

Table 13. EDX analysis results of the ettringite crystal from the second studied area at points 564, 566 and 568 from sample BI in Figure 7b, c and e after 121 days.

Point	564		566		568	
Element	**Mass %**	**Atomic %**	**Mass %**	**Atomic %**	**Mass %**	**Atomic %**
Al	1.464	1.212	0.702	0.825	1.329	1.736
Si	5.077	4.038	4.347	4.907	4.696	5.896
S	1.034	0.720	0.836	0.827	0.467	0.513
Ca	49.763	27.735	80.577	63.744	50.309	44.269

Table 14. EDX analysis results of the ettringite crystal from the first studied area at point 583 from sample BI-DT in Figure 9c after 121 days.

Element	Mass %	Atomic %
Al	5.970	6.509
Si	15.727	16.473
S	9.340	8.568
Ca	47.938	35.185

Table 15. EDX analysis results of the ettringite crystal from the second studied area at points 586, 587, 588 and 589 from sample BI-DT in Figures 10c, 10d, 10e and 10f after 121 days.

Point	586		587		588		589	
Element	**Mass %**	**Atomic %**	**Mass %**	**Atomic %**	**Mass %**	**Atomic %**	**Mass %**	**Atomic %**
Al	4.875	5.783	0.225	0.328	0.831	1.109	3.958	4.260
Si	11.808	13.457	1.148	1.607	4.107	5.264	11.331	11.718
S	4.657	4.648	0.960	1.177	0.897	1.006	5.384	4.876
Ca	62.473	49.892	95.707	93.929	82.188	73.815	57.537	41.696

induced nuclei created compressive stresses within the concrete matrix that then led to strength improvements as suggested by Springenschmid and Breitenbucher (1998).

Conclusion

DEF has been detected in all fine grained concrete prisms that were exposed to Duggan's test (B-DT and BI-DT). In addition, non-aerated fine grained concrete prisms B-DT show rapid and excessive increases in compressive strength, which leads to known harmful damages of hardened, concrete. Controlling DEF by using AEA as a nucleation agent results in a slight increase of compressive strength of fine grained concrete with only marginally lower density (comparison between BI-DT and BI). The detected ettringite crystals within the crystallisation nuclei prevented initial improvements of mechanical properties, which were observed in fine grained concrete B-DT without AEA as a result of excessive growth-related pressure on the walls of microcracks. This could be one of the reasons why air-entrained concrete normally does not suffer from DEF as reported by Hime (1996). The investigation shows that AEA-induced nucleation can prevent deterioration of hardened concrete and may even offer a mechanism for improvement of mechanical properties but further investigations over longer test periods are required to establish whether the deterioration can be completely avoided and whether such improvements can be achieved and sustained.

REFERENCES

ASTM C490-86, Standard Specifications for Apparatus for Use in Measurement of Length Change Of Hardenet Cement Paste, Mortar, and Concrete, American Society of Testing and Materials, 1986.

Barbarulo R, Peycelon H, Prené S, Marchand J (2005) Delayed ettringite formation symptoms on mortars induced by high temperature due to cement heat of hydration or late thermal cycle, Cem. Conc. Res. 35(1):125-131.

Bortolotti L (1994). Influence of concrete tensile ductility on compressive strength of confined columns, J. mater. civil eng. 6(4):542-564.

Brunetaud X, Divet L, Damidot D (2008). Impact of unrestrained Delayed Ettringite Formation-induced expansion on concrete mechanical properties, Cem. Conc. Res. 38(11):1343-1348.

Chrysochoou M, Dermatas D (2006). Evaluation of ettringite and hydrocalumite formation for heavy metal immobilization: Literature

review and experimental study, J. Hazardous Mater. 136(1):20-33.
Clifton JR, Ponnersheim JM (1994). Sulfate attack of cementitious materials: Volumetric relations and expansions. *NISTIR 5390*, US Department of Commerce.
Crawley WO (1953). Effect of Vibration on Air Content of Mass Concrete, ACI J. Proc. 49(6):909-920.
Collepardi M (2003). A state-of-the-art review on delayed ettringite attack on concrete, Cem. Conc. Composites 25(4-5):401-407.
Collepardi M (2001). Ettringite formation and sulfate attack on concrete. In: Proceedings of the 5th CANMET/ACI International Conference on Recent Advances in Concrete Technology, Singapore, pp. 27-39.
Cutler RA, Bright JD, Virkar AV, Shetty DK (1987). Strength improvement in transformation-toughened alumina by selective phase transformation, J. Am. Ceramic Soc. 70(10):714-718.
Diamond S (1996). Delayed ettringite formation - Processes and problems, Cem. Conc. Composites, 18(3):205-215.
Ekolu SO, Thomas MDA, Hooton RD (2007a). Dual effectiveness of lithium salt in controlling both delayed ettringite formation and ASR in concretes, Cem. Conc. Res. 37(6):942-947.
Ekolu SO, Thomas MDA, Hooton RD (2007b). Implications of pre-formed microcracking in relation to the theories of DEF mechanism, Cem. Conc. Res. 37(2):161-165.
EN 196-1:1999 Cement and concrete technology, Cements, Cement mortar, Compressive strength, Flexural strength, Compression testing, Bend testing, Compaction tests, Test equipment, Test specimens, Acceptance inspection, Conformity, Approval testing.
EN 197-1:2002 Cement – Part 1: Composition, specification and conformity criteria for common cements.
EN 450-1:2005 Fly ash, Concretes, Construction materials, Ashes, Chemical composition, Fineness, Density, Expansion (deformation), Marking, Quality control, Conformity, Sampling methods, Size classification, Defects, Statistical quality control, Power station waste aggregates.
Grabowski E, Czarnecki B, Gillott JE, Duggan CR, Scott JF (1992). Rapid test of concrete expansivity due to internal sulfate attack, ACI Mater. J. 89(5):469-480.
Hime WG (1996). Delayed ettringite formation – A concern for precast concrete? PCI Journal, July-August, 26-30.
Hover KC (2001). Vibration Tune-up, Conc. Int. 23(9):30-35.
Lawrence CD (1995a). Mortar expansions due to delayed ettringite formation. Effects of curing period and temperature, Cem. Conc. Res. 25(4):903-914.
Lawrence CD (1995b). Delayed ettringite formation: an issue? *Materials Science of Concrete*, vol. IV, American Ceramic Society, Ohio, USA, pp. 113-154.
Marshall DB, Ratto JJ, Lange FF (1991). Enhanced Fracture Toughness in Layered Microcomposites of Ce-ZrO_2 and Al_2O_3, J. Am. Ceramic Soc. 74(12):2979-2987.
Mather B (1968). Field and Laboratory Studies of the Sulphate Resistance of Concrete, Performance of Concrete-Resistance of Concrete to Sulphate and Other Environmental Conditions, Thorvaldson Symposium Proceedings, University of Toronto Press, Toronto, pp. 66-76.
Mehta PK (1983). Mechanism of sulfate attack on Portland cement concrete-another look, Cem. Conc. Res. 13(3):401-406.
Mishnaevsky L Jr (2007). Computational Mesomechanics of Composites, John Wiley. 74(12):2979-2987.
Myneni SCB, Traina SJ, Logan TJ, Waychunas GA (1997). Oxyanion behavior in alkaline environments: Sorption and desorption of arsenate in ettringite, Environ. Sci. Tech. 31:1761–1768.
Richardson IG (2000). The nature of the hydration products in hardened cement pastes, Cem. Conc. Composites, 22(2):97-113.
Rothstein D, Thomas JJ, Christensen BJ, Jennings HM (2002). Solubility behaviour of Ca-, S-, Al-, and Si-bearing solid phases in Portland cement pore solutions as a function of hydration time, Cem. Conc. Res. 32(10):1663-1671.
Ryu JS, Otsuki N (2002). Crack closure of reinforced concrete by electrodeposition technique, Cem. Conc. Res. 32(1):159-164.
Sahu S, Thaulow N (2004). Delayed ettringite formation in Swedish concrete railroad ties, Cem. Conc. Res. 34(9):1675-1681.
Sobolev K, Flores I, Hermosillo R, Torres-Martinez LM (2006). Nanomaterials and nanotechnology for high-performance cement composites, Proceedings of ACI Session on “Nanotechnology of Concrete: Recent Developments and Future perspectives”, November 7, Denver, USA.
Springenschmid R, Breitenbucher R (1998). Influence of constituents, mix proportions and temperature on cracking sensitivity of concrete. In Springenschmid R (1998). Prevention of thermal cracking in concrete at early stages. RILEM Report 15, E & FN Spon.
Swaddiwudhipong S, Chen D, Zhang MH (2002). Simulation of the exothermic hydration process of Portland cement, Adv. Cem. Res. 14(2):61-69.
Taylor HFW (1990). Cement Chemistry, Academic Press, London, England.
Thomas MDA (2001). Delayed ettringite formation: Recent developments and future directions, in: S. Mindess, J. Skalny (Eds.), Materials Science of Concrete VI, American Ceramics Society, Westerville, OH, 2001, pp. 435–482.
Thomas M, Folliard K, Drimalas T, Ramlochan T (2008). Diagnosing delayed ettringite formation in concrete structures, Cem. Conc. Res. 38:841-847.
Ozyldirim C, Lane DS (2003). Investigation of self-consolidating concrete, Transportation Research Board Annual Meeting, National Research Council.
Solem JK, McCarthy GJ (1992). Hydration reactions and ettringite formation in selected cementitious coal conversion byproducts, Mater. Res. Soc. Symposium Proc. 245:71-79.
Stang H (1996). Significance of shrinkage – induced clamping pressure in fiber matrix bonding in cementitious materials, Adv. Cem. Based Mater. 4(3):106-115
Zhang M, Jiang M, Chen J (2008). Variation of flexural strength of cement mortar attacked by sulfate ions. Eng. Fracture Mechan. 75(17):4948-4957.
Zhang M, Reardon EJ (2003). Removal of B, Cr, Mo, and Se from wastewater by incorporation into hydrocalumite and ettringite, Environ. Sci. Technol. 37(15):2947-2952.
Xu A, Sarkar SL, Nilsson LO (1993). Effect of fly ash on the microstructure of cement mortar, Mater. Structures 26(7):414-424.